**Journal of NeuroVirology,** 13: 185–194, 2007

ISSN: 1355-0284 print / 1538-2443 online
DOI: 10.1080/13550280701258415

informa
healthcare

# Neonatal Borna disease virus infection in rats is associated with increased extracellular levels of glutamate and neurodegeneration in the striatum

Mikhail V Ovanesov,[1,2] Michael W Vogel,[3] Timothy H Moran,[2] and Mikhail V Pletnikov[1,2]

*[1]Division of Neurobiology, and [2]Department of Psychiatry and Behavioral Sciences, Johns Hopkins University, Baltimore, Maryland, USA; [3]Maryland Psychiatric Research Center, University of Maryland, Catonsville, Maryland, USA*

**The authors evaluated a role of glutamate (GLU) excitotoxicity in neonatal Borna disease virus (BDV) infection–associated neuronal injury by measuring extracellular levels of GLU in the striatum of 70-day-old Fischer344 rats using *in vivo* microdialysis. The effects of BDV infection on the protein levels of the GLU transporters and the cystine-GLU antiporter and on the total numbers of striatal neurons and the volume of the striatum were also assessed. BDV increased the basal levels of GLU but did not change those of aspartate, glutamine, or taurine. BDV infection did not alter the effects of a blockade of GLU transporters but attenuated the effects of an inhibition of the cystine-GLU antiporter, without affecting the protein levels of the GLU transporters. The elevated levels of GLU were associated with decreased neuronal numbers and volume in the striatum. The present data are the first *in vivo* evidence that GLU excitotoxicity might contribute to BDV-associated neuronal injury in the striatum.** *Journal of NeuroVirology* (2007) **13,** 185–194.

**Keywords:** Borna; glutamate; microdialysis; neurodegeneration; striatum

## Introduction

Borna disease virus (BDV) is a nonsegmented negative-strand RNA virus that persistently infects the central nervous system (CNS) and causes behavioral abnormalities in a broad spectrum of warm-blooded animals (Richt and Rott, 2001; de la Torre, 2002). Experimental BDV infection in adult rats produces a mononuclear inflammatory reaction in the CNS and peripheral nervous system with severe perivascular cuffing of T cells and macrophages (Briese *et al*, 1999; Richt *et al*, 2001; Gonzalez-Dunia *et al*, 1997). In contrast, BDV infection in neonatal rats causes a life-long persistent infection of the CNS with minimal signs of infiltration of inflammatory cells (Pletnikov *et al*, 2002a; de la Torre, 2002). Nevertheless, neonatal BDV infection is associated with progressive loss of granule cells in the dentate gyrus of the hippocampus, Purkinje cells in the cerebellum, and $\gamma$-aminobutyric acid (GABA)-ergic neurons in the neocortex (Bautista *et al*, 1995; Carbone *et al*, 1991; Eisenman *et al*, 1999; Gonzalez-Dunia *et al*, 2000; Hornig *et al*, 1999; Pletnikov *et al*, 2002b). Neuronal loss in other brain regions following neonatal BDV infection has not been quantitatively assessed, although this possibility has been suggested (Weissenböck *et al*, 2000; Williams and Lipkin, 2006).

The mechanisms of BDV-associated neuronal injury remain unclear (Gonzalez-Dunia *et al*, 2005). Because BDV establishes persistent noncytotoxic infection in various cell lines and primary neurons and astrocytes *in vitro* (Tomonaga *et al*, 2002; de la Torre, 2002), the observed neuronal degeneration *in vivo* has been postulated to occur via

Address correspondence to Mikhail V. Pletnikov, MD, PhD, Division of Neurobiology, Department of Psychiatry and Behavioral Sciences, Johns Hopkins School of Medicine, 600 North Wolfe Street, CMSC 8-121, Baltimore, MD 21287, USA. E-mail: mpletnik@jhmi.edu

The authors would like to thank Dr. Thomas Guilarte (JHU Bloomberg School of Public Health) for his generous help with the microdialysis equipment. The authors are grateful to Steven Rubin, MA, and Christian Sauder, PhD (U.S. Food and Drug Administration, Center for Biologics Evaluation and Research, Bethesda, MD) for helpful comments on the revised manuscript. This study was supported by R01MH048948.

Received 5 November 2006; revised 10 January 2007; accepted 23 January 2007.

indirect, glia-mediated mechanisms (Hornig *et al*, 1999, Sauder and de la Torre, 1999; Weissenböck *et al*, 2000). Indeed, strong microgliosis and astrocytosis have been found predominantly in the areas of significant neuronal loss, i.e., the cortex, hippocampus, and cerebellum (Sauder and de la Torre, 1999; Weissenböck *et al*, 2000). Once activated, glia cells may produce various neurotoxins, including glutamate (GLU) and quinolinic acid, which are direct excitotoxins (Hara and Snyder, 2006; Kaul and Lipton, 2006), and arachidonic acid and nitric oxide, which may act as indirect excitotoxins by suppressing GLU reuptake (Danbolt, 2001, Maragakis and Rothstein, 2004). A contribution of GLU excitotoxicity to BDV neuropathology was first proposed by Gosztonyi and Ludwig (1984). The group postulated that a subtype of GLU receptors, kainate 1 receptors, is the BDV receptor within the CNS and binding of the virus to the receptor might lead to dysfunctional GLU neurotransmission in the hippocampus (Gosztonyi and Ludwig 1995, 2001). Direct BDV infection of primary feline astrocytes *in vitro* has been shown to inhibit GLU re-uptake, suggesting another potential mechanism of excitotoxic injury of neurons (Billaud *et al*, 2000). BDV-associated alterations in expression of $\alpha$-amino-3-hydroxy-5-methylisoxazole-4-propionic acid (AMPA) receptors in the cerebellum might also contribute to the loss of Purkinje cells (Hornig *et al*, 2001).

However, all of the available evidence supporting the role for GLU excitotoxicity in the BDV neuropathogenesis is indirect. Thus, the present study sought to directly measure extracellular levels of GLU in the striatum *in vivo*. The striatum was chosen for several reasons. Because a substantial inhibition of GLU uptake has not been observed until 2 to 3 months after persistent BDV infection of astrocytes (Billaud *et al*, 2000), we reasoned that GLU levels should be measured in 2- to 3-month-old rats to provide a sufficient time for inhibition of GLU uptake to develop. Thus, we chose the striatum because it is relatively spared by the end of the 2nd postnatal month, making it possible to measure extracellular levels of GLU without the confounding effects of prior neurodegeneration (Gonzalez-Dunia *et al*, 2005). In contrast, measuring levels of GLU in the hippocampus of 2-month-old rats was reasoned to be less informative for understanding of putative effects of GLU excitotoxicity on cell death because of dramatic degeneration of the dentate gyrus by the end of the 1st postnatal month (Dietz *et al*, 2004). In addition, evaluating BDV-associated alterations in levels of extracellular GLU was thought to be more feasible in the striatum because the sources of extracellular GLU in that brain region have been recently studied in more details compared to other brain areas (Baker *et al*, 2002).

The extrasynaptic concentrations of GLU measured by microdialysis are determined by the balance of nonvesicular release and reuptake (clearance) mechanisms (Nyitrai *et al*, 2006; Timmerman and Westerink, 1997). The cystine-GLU antiporter (CG antiporter or the $X_c^-$ exchanger) has been shown to be a major source of extracellular GLU in the striatum (Baker *et al*, 2002; McBean, 2002), whereas clearance of GLU is accomplished by the astrocyte reuptake mechanisms (Maragakis and Rothstein, 2004). Thus, in addition to analyzing striatal GLU levels, we also analyzed the effects of BDV infection on the activity of the cystine-GLU antiporter (a main source of extracellular GLU in the striatum) and the astrocyte GLU transporters (the clearance mechanisms) by measuring levels of GLU after pharmacological blockage of the CG antiporter or the astrocyte GLU transporters. The protein levels of the CG antiporter and the GLU transporters, GLT-1 and GLAST, were measured by Western blot and the number of striatal neurons and volume were estimated by stereological techniques. We found that neonatally BDV-infected 70-day-old Fischer344 rats had a significant elevation of extracellular GLU and altered responses to blockade of the CG antiporter. In addition, neonatal BDV infection led to a significant decrease in the total number of striatal neurons and the volume of the striatum. The present findings are the first *in vivo* evidence for a BDV-associated elevation of GLU levels and neuronal degeneration in the striatum.

## Results

### *Amino acid concentrations in dialysates from striatum*

Neonatal BDV infection was associated with a significant increase in the extracellular levels of GLU in the striatum ($P < .05$; Table 1), whereas there were no significant BDV-induced changes in the levels of aspartate, glutamine or taurine (Table 1).

### *Effects of PDC on levels of GLU*

In order to evaluate the effects of neonatal BDV infection on the GLU transporters, we used reverse dialysis to apply different concentrations of a competitive inhibitor of the GLU transporters, L-*trans*-2,4-pyrrolidine dicarboxylate (PDC), that increases extracellular levels of GLU by competitively inhibiting uptake and heteroexchange with cytoplasmic GLU stores (Danbolt, 2001). In order to reduce the variability in the extracellular levels of GLU, we coapplied

**Table 1** The effects of neonatal BDV infection on the extracellular levels of glutamate, aspartate, glutamine, and taurine in the striatum

| Amino acid (pmoles/sample) | Control | BDV |
|---|---|---|
| Glutamate | $13.2 \pm 2.4$ | $30.4 \pm 6.6^*$ |
| Aspartate | $13.1 \pm 3.8$ | $13.8 \pm 3.5$ |
| Glutamine | $92.3 \pm 35$ | $69.8 \pm 20$ |
| Taurine | $27.7 \pm 6.8$ | $15.4 \pm 7.6$ |

*Note*. The data are presented as the mean ± SEM.
$^*P < .05$ versus the control group for glutamate.

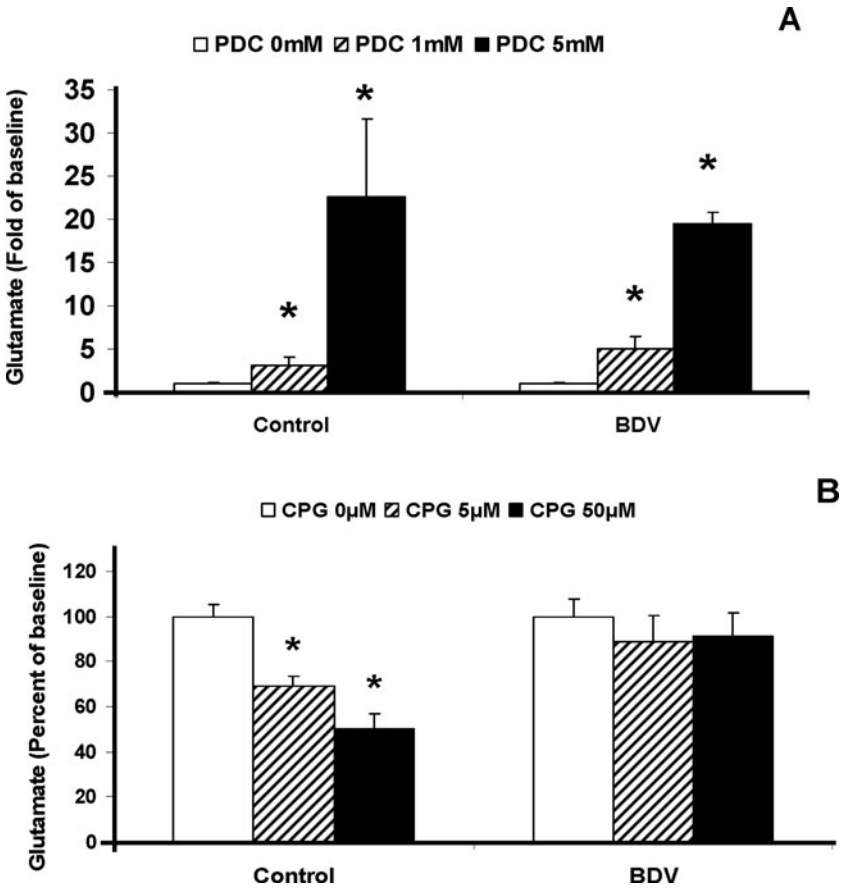


**Figure 1** The effects of neonatal BDV infection on the extracellular levels of GLU following reverse dialysis of different doses of PDC (**A**) or CPG (**B**) in the striatum. Note the comparable dose-dependent increases of GLU levels in the perfusates in both groups of rats after reverse dialysis of PDC, all $P < .05$ versus PDC 0 mM in the same group. In contrast, there were no significant inhibitory effects of CPG in the neonatally BDV-infected rats as compared to the dose-dependent decrease in the levels of GLU in the control animals. $^{*}P < .05$ versus CPG 0 $\mu$M in the same group.

PDC with high concentrations of KCl that depolarizes neurons and releases the vesicular pool of amino acids in a calcium-dependent process (Espey *et al*, 1998). Coapplications of PDC at doses of 1 and 5 mM in the dialysate buffer containing 100 mM KCl evoked comparable and significant dose-dependent increases in the extracellular levels of GLU in the control and BDV-infected rats (Figure 1A).

*Effects of CPG on levels of GLU*

One of the sources of extracellular GLU in the brain has been shown to be the CG antiporter that transports cystine into the cell in a 1:1 exchange for GLU, which travels outwards down its concentration gradient (McBean, 2002). In order to evaluate the effects of neonatal BDV infection on activity of the CG antiporter system, we blocked activity of the CG antiporter with reverse dialysis of (***S***)-4-carboxyphenylglycine (CPG), an inhibitor that blocks both cystine uptake and GLU release (McBean, 2002). We found that reverse dialysis of CPG led to a dose-dependent decrease of the extracellular levels of GLU in the striatum of control rats. In contrast, applications of CPG did not alter the extracellular levels of GLU in striatum of the neonatally BDV-infected rats (Figure 1B). An analysis of the data for the levels of GLU in the control rats showed a significant effect of dose $F(2, 14) = 12.2$, $P < .01$. *Post hoc* comparisons demonstrated a significant decrease of the levels of GLU in striatum after reverse dialysis of 5 and 50 $\mu$M of CPG, $P < .05$. In contrast, the analysis found no effects of CPG on the GLU levels in the striatum of the BDV-infected rats, $P > .05$.

*Expression of GLU transporters in striatum*

The effects of neonatal BDV infection on the expression of the GLU transporters were determined by Western blotting technique (Figure 2A). We evaluated the expression of GLAST, GLT-1, and the light chain of the CG antiporter (known as xCT, the $X_c^-$ transporter related protein; 502 amino acids) (McBean, 2002; Melendez *et al*, 2005). No statistically significant effects of BDV infection on the protein levels of either transporter were noted (Figure 2B). The Western blotting data demonstrated that the striatal samples from the BDV-infected rats were positive for p40, whereas no positive staining was found in the samples from the control rats (Figure 2A, *bottom panel*).

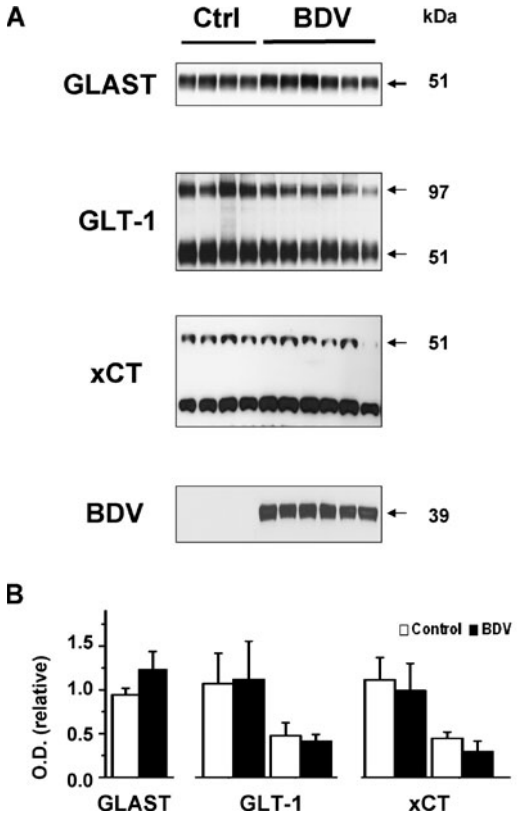


**Figure 2** There are no changes in the concentration of GLAST, GLT-1, and xCT (the light chain of the CG antiporter) proteins in the striatum in response to neonatal BDV infection. All the brain samples from the BDV-infected rats were also positive for the BDV N protein (**A**, *bottom panel*). Arrows point to the specific bands for each GLU transporter or the N BDV protein (*bottom blot*). The analysis of the protein levels found no differences between the groups in either transporter, all $P > .05$ (**B**). Proteins GLT-1 and xCT appeared as two clear bands on Western blots, thus, comparative analyses of the band intensities between the groups were performed independently for each band (**B**) or two bands combined (data not shown); all the analyses gave $P > .05$.

*BDV infection of neurons, astrocytes and associated astrocytosis and microgliosis*

In order to assess levels of astrocytosis and microgliosis in the striatum of BDV-infected rats, we performed immunostaining of brain sections from the control and BDV-infected rats. We found a dramatic increase in ED1-positive and Glial Fibrillary Acidic Protein (GFAP)-positive staining in the BDV-infected rats (Figure 3C, G) compared to control animals (Figure 3D, H). Many of GFAP-positive cells were also positive for BDV nucleoprotein (yellow staining) (Figure 3G, *inset*). We found that 18.1% ± 2.7% of calbindin-positive neurons were infected with the virus (Figure 3K and *inset*).

*Effects of BDV on the striatal volume and the number of neurons*

An analysis of the quantitative data showed a significant decline in the total number of striatal neurons (Figure 4A), $P < .01$, and a significant decrease in the volume of the striatum in the BDV-infected rats compared to the control animals, $p < .01$ (Figure 4B). The estimates for striatal neuron numbers and the percent decline in striatal volume did not differ between brains processed for paraffin or frozen sections.

## Discussion

The novel findings of the study are neonatal BDV infection-associated elevation of extracellular levels of GLU and neurodegeneration in the striatum of adult rats.

The study is the first *in vivo* report to directly demonstrate that neonatal BDV infection produces increased extracellular concentrations of GLU in the striatum. Given that BDV infection is present in astrocytes by the end of the second postnatal month, one can hypothesize that increased levels of GLU in the striatum are due to decreased GLU reuptake. This would be consistent with a study by Billaud *et al* demonstrating that persistent BDV infection of primary cortical feline astrocytes leads to a significant inhibition of GLU reuptake (Billaud *et al*, 2000). We did not find any significant effects of neonatal BDV infection on the expression of GLT-1 or GLAST or the pharmacological blockade of GLU transporters. Nevertheless, BDV-associated changes in the activity of those transporters cannot be ruled out. For example, a similar discrepancy between the absence of alterations in the expression of GLT-1 and elevated levels of extracellular GLU has been found in transgenic mice expressing human mutant (G93A) Cu/Zn superoxide dismutase (Alexander *et al*, 2000).

In addition to a putative decrease in GLU re-uptake in the BDV-infected rats, it is conceivable that the elevated levels of extracellular GLU could result from a virus-associated increase in GLU release from a number of potential sources (Anderson and Swanson, 2000; Danbolt, 2001). In many pathological conditions, astrocytic swelling has been shown to be followed by a volume decrease driven by $Na^+$, water, and GLU efflux. However, our results do not support this mechanism. Indeed, swelling-associated GLU efflux is coupled with the release of taurine, an important CNS osmoregulator, into the extracellular space (Pasantes-Morales, 1996). Because we did not observe any significant changes in the levels of taurine, the increased levels of GLU levels were unlikely produced by astrocytic swelling.

Recent studies have suggested that the CG antiporter may be a primary source of extracellular GLU in the striatum (Baker *et al*, 2002). We found that blockage of the antiporter by reverse dialysis of CPG, a selective nontransportable inhibitor of the antiporter, produced a dose-dependent decrease (up to 60%) in the GLU levels in the control rats. In contrast, no CPG-related changes in the GLU levels were observed in the BDV-infected rats. The attenuated effects of CPG on GLU levels in the BDV-infected rats

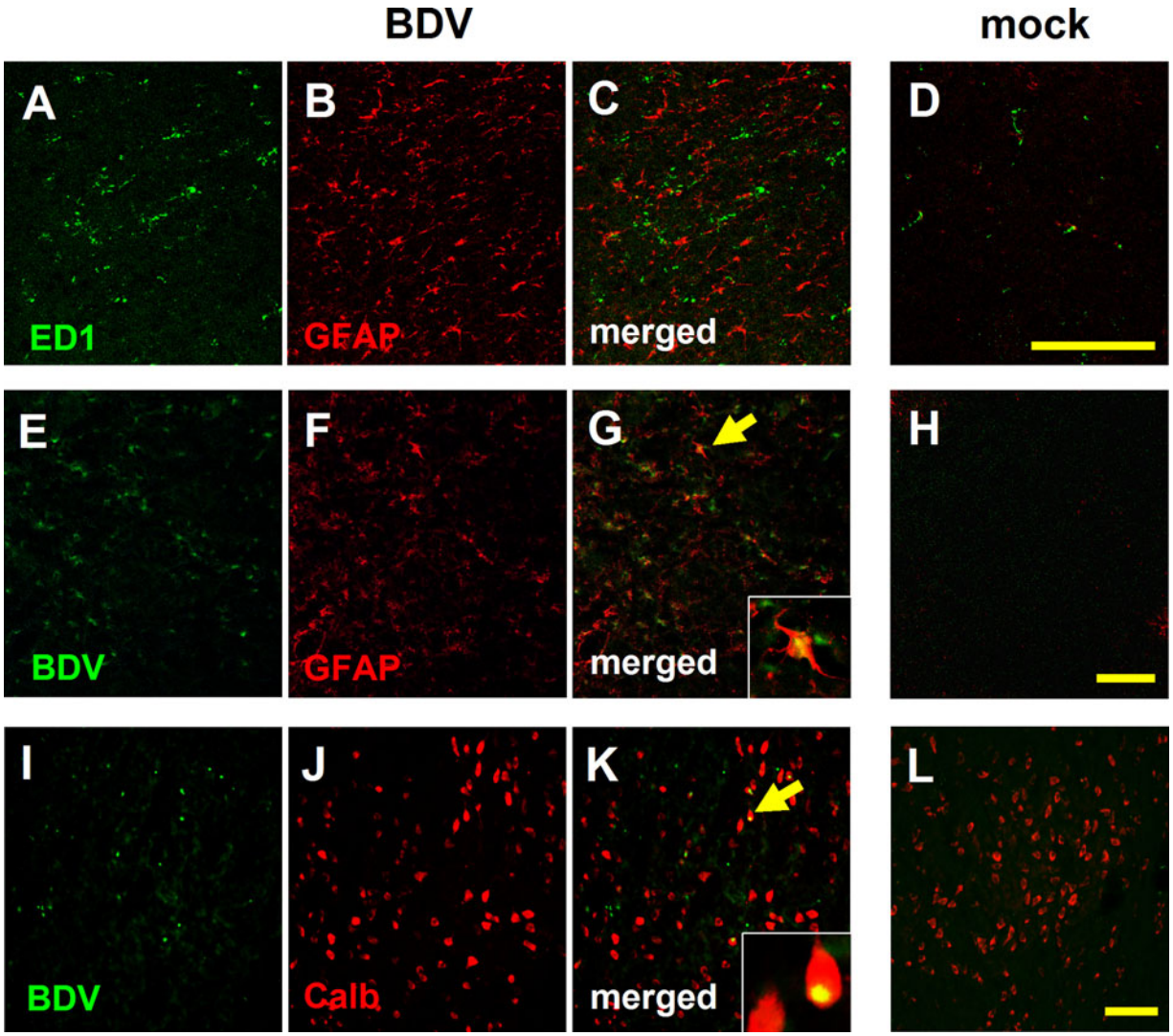


**Figure 3** Microgliosis, astrocytosis, and BDV infection of neurons and astrocytes in striatum of BDV-infected and control animals are shown on representative images from a BDV-infected (**A, B, C, E, F, G, I, J, K**) and control rat (**D, H, L**). Activated microlglia are visualized with ED1 (*green,* **A, C, D**). Note the BDV-associated microglia activation (**A** and **C** versus **D**). Astrocytes are labeled with anti-GFAP (*red,* **B, C, F, G**). Note astrocytosis in a BDV-infected brain (**F**) compared to a control one (**H**). Some astrocytes in the BDV-infected striatum were also positive for the BDV N protein (*green*, **E, G**). The arrow (**G**) points to a BDV-infected astrocyte double positive for GFAP and BDV N protein. This double-stained cell is also presented in the inset of panel **G** (*yellow staining*). About 20% of calbindin-positive neurons (**J**) in the striatum were infected with BDV (**I, K**). The arrow (K) points to a BDV-infected neuron double positive for BDV (*green*) and calbindin (*red*). The inset of panel **K** presents this neuron (*yellow staining*). Scale bars are 100 $\mu$m.

could be due to a number of possibilities. Because the CG antiporter has been shown to be mainly localized to glial cells (Baker *et al*, 2002; Danbolt, 2001), one can hypothesize that BDV-induced microgliosis and astrocytosis may be associated with a BDV-induced increase in the expression of the CG antiporters, giving rise to attenuation of the effects of CPG. However, our results do not support this hypothesis because we found no differences in the protein levels of the antiporter between the control and BDV-infected rats. Alternatively, the weak effects of CPG on the GLU levels in the BDV-infected rats may be related to changes in the activity of the CG antiporter due to altered phosphorylation of xCT monomer of the CG antiporter (Gochenauer and Robinson, 2001, Tang and Kalivas, 2003) or the inhibition of the heterodimer formation (Melendez *et al*, 2005). The latter mechanism would be in line with our observation of unchanged protein levels of the CG antiporter light chain (i.e., xCT monomer).

It is also possible that the elevated extracellular levels of GLU in the BDV-infected rats could be in part related to a source that cannot be inhibited by blockage of the CG antiporter. For example, BDV infection of astrocytes could induce secretion of GLU by astrocytes by reversing the electrochemical gradients across the cell membranes and leading to GLU release instead of uptake. An excessive release of GLU into the extracellular space could also occur via the poorly characterized vesicular glutamate transporter

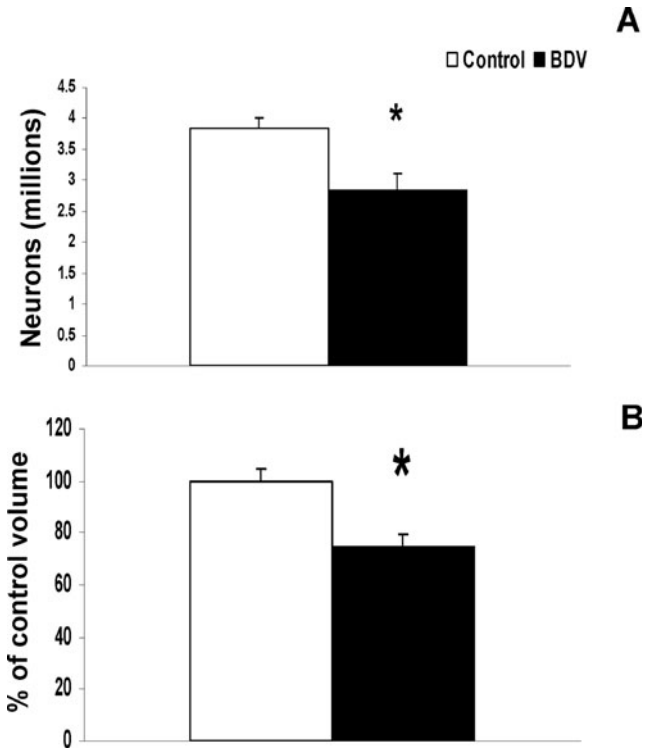


**Figure 4** The effects of neonatal BDV infection on the total number of neurons **(A)** and the volume **(B)** of the striatum. Note a significant decline in the total number of striatal neurons and a significant decrease in the relative volume of the striatum in the BDV-infected rats compared to the control animals. $^{*}P < .01$ versus control, Student *t* test.

or other transmembrane diffusion processes postulated to permit diffusion of GLU into the extracellular space (Danbolt, 2001). Future *in vitro* experiments may shed more light on specific sources of extracellular GLU in BDV-infected brains.

Although our data do not provide direct evidence of GLU excitotoxicity in the striatum, it is tempting to speculate that the elevation of GLU in BDV-infected rats might be responsible for the loss or decreased survival of neurons in the striatum. This hypothesis is based on the fact that 95% of striatal neurons are projection GABA medium spiny neurons that are particularly susceptible to GLU excitotoxicity (Mitchell *et al*, 1999). Future studies with blockade of GLU NMDA receptors and counting neurons at different time points may help to directly demonstrate the causative relationship.

GLU excitotoxicity has been predominantly described for acute overstimulation of GLU receptors—so called fast excitotoxicity or direct excitotoxicity. In contrast, more subtle and chronic forms of excitotoxicity *in vivo* remain poorly understood despite the fact that they appear to be more relevant to the mechanisms of slowly evolving neuronal degenerative conditions, including persistent neurotropic virus infections (Sonsalla *et al*, 1998). In this context, the BDV rat model provides a valuable experimental system to study the effects of chronic elevation of extracellular GLU on neuronal functioning and survival.

In conclusion, neonatal BDV infection in the striatum was associated with a significant elevation of extracellular GLU, alterations in the activity of the CG antiporter, and a decrease in the total number of striatal neurons and striatal volume. No BDV-associated changes were found in the protein levels of the CG antiporter, GLT-1 or GLAST. The present data suggest that GLU excitotoxicity might contribute to neuronal loss following neonatal BDV infection.

## Materials and Methods

*Animals*

Pregnant Fischer344 rats at 16 to 18 days of gestation were purchased for the present study (Harlan, Indianapolis, IN). All rat pups were born in the animal facility at Johns Hopkins University School of Medicine, Baltimore, MD. Mothers and their litters were housed in 45 × 26 × 23-cm pan-type polypropylene cages with paper-chip bedding and an overhead wire grid supporting food pellets and a water bottle. The cages containing BDV-infected animals were kept in a DUO-FLO biosafety cabinet (Bio-Clean Lab Product, NJ). The sham-inoculated rats were kept in the same room. Rats of all the groups were maintained on a 12/12-h light/dark cycle (lights on at 8 AM). Room temperature was maintained at approximately 21°C. The pregnant and nursing rats had free access to food and water. After weaning, on postnatal day 23, the rats continued to have free access to food and water.

*Inoculation*

The rat pups were inoculated intracranially under hypothermia anesthesia with 26-G needles within 24 h of birth either with 0.02 ml of infectious inoculum containing $10^4$ $TCID_{50}$ of He-80 BDV strain or 0.02 ml of uninfected inoculum as described previously (Carbone *et al*, 1991). For intracranial inoculation, a rat pup was taken out of the home cage and placed on ice. After an injection, the rat pup was warmed with a warm cloth, and returned to the home cage. BDV stock was prepared from homogenized BDV-infected rat brain tissue as described earlier (Carbone *et al*, 1991). No more than one male rat was used from a single litter to compose each experimental group.

*Surgery*

At postnatal day (PND) 70, the control ($n=6$) and BDV-infected ($n=6$) rats included in the microdialysis study were anesthetized with a combination of ketamine (100 mg/kg, intramuscular [i.m.]) and xylazine (3 mg/kg, i.m.). Guide cannulae were implanted above the striatum to allow the microdialysis probes (CMA 12; CMA, Acton, MA) to be placed in the target area. The coordinates for cannula

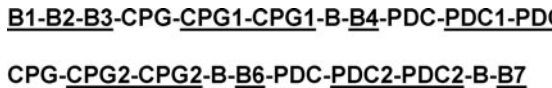


**Figure 5** Scheme of the typical microdialysis experiment B = the basal buffer; CPG = the buffer with (*S*)-4-carboxyphenylglycine, an inhibitor of the CG antiporter; PDC = the buffer with L-trans-2-4-pyrrolidine dicarboxylate, an inhibitor of the $Na^+$-dependent GLU transporters. Underlined B's with numbers show the collected basal perfusates. Underlined CPG's and PDC's with numbers show the collected perfusates for a given dose (e.g., 1 or 2 corresponds to 5 or 50 $\mu$M of CPG or PDC) of each drug. Each perfusate was collected for 20 min, B's, CPG's, and PDC's without numbers indicate what type of buffer was infused for 30 min between collections of the perfusates.

placement were taken from the rat brain atlas (Paxinos and Watson, 1998) (plate 14: lateral 2.5 mm; bregma +1.0; and −3.0 mm from the surface of the skull), taking into consideration that the microdialysis probe extends 4 mm beyond the tip of the guide cannula by 4 mm. Guide cannulae were secured to the skull using skull screws (Small Parts, Roanoke, VA) and dental acrylic. After surgery, the rats were given at least 5 days to recover before testing.

*In vivo microdialysis*

On the day of each experiment, a microdialysis probe (membrane, 4 × 0.24 mm, 6000 molecular weight cutoff, CMA 12; CMA) was inserted through the guide cannulas into the striatum. The dialysis buffer (5 mM glucose, 140 mM $Na^+$, 2.7 mM $K^+$, 1.4 mM $Ca^{2+}$, 0.83 mM $Mg^+$, 5.8 mM $H_2PO_4^+$, 0.8 mM $HPO_4^{2+}$, 20 mM $HCO_4^-$; pH 7.4) was pumped at a rate of 0.2 $\mu$l/min for at least 6 h (CMA 100 microdialysis pump). One hour before each microdialysis experiment, the rate was set at 1.0 $\mu$l/min. A zero-dead-volume liquid switch (CMA 110) was used to minimize pressure fluctuations while changing dialysis buffers with varying concentrations of the drugs. (***S***)-4-carboxyphenylglycine (CPG), an inhibitor of the CG antiporter, and L-*trans*-2,4-pyrrolidine dicarboxylate (PDC), an inhibitor of the GLU $Na^+$-dependent transporters (Tocris-Cookson, Ballwin, MO) were dissolved in 1 equivalent NaOH, diluted in the dialysis buffer, and infused into the probes via reverse dialysis. The standard protocol used for the microdialysis experiments is presented on Figure 5. The order of the drugs and their doses was counterbalanced across the rats. The concentrations of PDC (1 and 5 mM) and CPG (5 and 50 $\mu$M) were selected from previous microdialysis studies (Espey *et al*, 1998; Baker *et al*, 2002).

*Amino acid determination*

Microdialysis samples analyzed for glutamate (GLU), aspartate (ASP), glutamine (GLN) and taurine (TAU) were collected into vials containing 0.1 N $HClO_4$. The concentrations of amino acids in the dialysis samples were determined using reverse-phase high-performance liquid chromatography (HPLC) coupled to a LC-4B electrochemical detector (BAS, West Lafayette, IN). The glassy carbon electrode was set at a potential +0.75 V. The dialysis samples were derivatized with 1,2-phthalic dicarboxaldehyde (OPA) (ACROS) and injected into the mobile phase using a Waters autosampler 700 (Waters, Nautik, MA). A stainless steel column (Luna, C18-(2) 75 × 4.6 × 3 $\mu$; Phenomenex, Torrance, CA) protected by a guard column (Security Guard; Phenomenex) was used. The mobile phase consisted of 20 mM sodium dihydrogenphosphate and 10 mM disodium hydrogenphosphate, 21% methanol (pH 6.47), and was delivered at a flow-rate of 1.0 ml/min at room temperature. The concentration of amino acids was quantified by comparing peak heights from samples and external standards.

*Standards and reagents*

Stock solutions of individual amino acids were prepared in 0.1 N $HClO_4$ and appropriately diluted to make external standards in a range of 2.0 to 70 $\mu$M. The OPA–2-mercaproethanol (BME) stock reagent was prepared as follows: 27 mg of OPA was dissolved in 1 ml of methanol and 5 $\mu$l of BME followed by dissolving in 9 ml of 100 mM sodium borate. The working OPA-BME reagent was prepared daily by diluting the OPA stock solution in 100 mM sodium borate (1:3 *v*/*v*). For preparing derivatives, a 10-$\mu$l aliquot of dialysis sample was automatically mixed with 8 $\mu$l of OPA-BME working solution at room temperature, and exactly after 3 min, 10 $\mu$l of the resultant mixture were injected into the HPLC system.

*Probe placement verification and immunohistochemistry*

Upon completion of the dialysis experiments, control and BDV-infected rats were euthanized with EUTHASOL (Diamond Animal Health, IA) and perfused with phosphate-buffered saline (PBS; pH = 7.4), followed by 4% paraformaldehyde. Brains were removed, postfixed for 4 h, cryoprotected, and cut sagittally in half. The half of the brain that had the guide cannula inserted was cut coronally in 20-$\mu$m sections, lightly stained with cresyl violet to verify the cannule placement. The other half was cut coronally in 12-$\mu$m sections for immunostaining. Brains sections were costained with rabbit anti-GFAP (1:800; Chemicon, Temecula, CA), anti-ED1 monoclonal antibodies (mAbs) (1:100; Chemicon) and anti-BDV N Mo18 mAbs (1:100; a generous gift by Dr. Juergen Richt, National Animal Disease Center, Ames, IA) (Haas et al, 1986), rabbit anti-calbindin (a marker of GABA-ergic neurons; 1:200; Chemicon) antibodies followed by either flurescein isothiocyanate (FITC)-conjugated or Cy3-conjugated secondary antibodies (1:200; Chemicon). Images were viewed on Zeiss confocal microscope (Axioskop 2; LSM 5 PASCAL). Semiquantitative estimation of the percentage of BDV-positive neurons was performed by counting double-stained cells in microscopic fields randomly sampled from

the BDV-infected sections. At least six sections from each BDV-infected rat were analyzed. The data are presented as the mean ± SEM.

*Western blotting assay*

For this assay, separate control ($n=4$) and BDV-infected ($n=6$) 70-day-old Fischer344 rats were used. Tissue preparation was done according to Deitch *et al* with minor modifications (Deitch *et al*, 2002). The striatum from each brain was quickly dissected out in ice-cold PBS, frozen on dry ice, and kept at −80°C until used. Brain tissue was homogenized in 10 parts buffer (10 mM Tris, pH 8.0, 1 mM EDTA, 0.32 M sucrose) using manual sonicator (with two 6-s pulses). The homogenate was centrifuged at $10000 \times g$ for 15 min, the supernatant collected, combined with an equal volume of 2× sample buffer (1× concentrations: 62.5 mM Tris, pH 8.0, 5% sodium dodecyl sulfate [SDS], 5% glycerol), and boiled for 5 min at 95°C. An aliquot was taken for BCA (bicinchoninic acid) protein assay (Pierce Biotechnology, Rockford, IL).

Samples from each specimen were combined with 4 × LDS sample buffer (Invitrogen), boiled for 5 min at 95°C, separated on a 10% Bis-Tris gel (Invitrogen) at 10 $\mu$g per lane, transferred to nitrocellulose membrane, and immunoblotted with antibodies to xCT, the light chain (i.e., 502 amino acids) of the CG antiporter (McBean, 2002) (1:800; TransGenic, Kumamoto, Japan). Labeling was visualized with a horseradish peroxidase (HRP)-conjugated anti-rabbit immunoglobulin G (IgG) antibody (1:5000; Amersham, Piscataway, NJ) and chemiluminescence (Pierce), and recorded on film at two or more exposure times. Thereafter, blots were stripped once with ReBlot Plus Strong Antibody Stripping Solution (Chemicon), and reprobed with one of the following glutamate transporter antibodies, GLT-1 or GLAST (1:20,000 each; Chemicon), and with loading control antibody (glyceraldehyde-3-phosphate dehydrogenase (GAPDH) 1:10000), followed by incubation with an HRP-conjugated anti–guinea pig IgG antibody (1:10 000; Chemicon). Films were digitally scanned and densitometric analysis of the Western blot images with bands that were below the saturation of the film was performed with ImageJ software (W. S. Rasband, ImageJ; U.S. National Institutes of Health, Bethesda, MD; http://rsb.info.nih.gov/ij/). For statistical analysis, 8 gels, each with 8 to 10 brain samples run in parallel, were used. The optical density of protein bands on each of digital images was normalized to the optical density of corresponding loading control (GAPDH), and then normalized to the optical density of sample from normal animal 1 (internal reference control). Thereafter, normalized protein content of glutamate transporters GLT1, GLAST, and xCT in each of four normal and six infected brain samples was calculated by combining data from independent measurements ($n=2$ or 3 per sample).

*Stereology-based count of neurons in the striatum*

For the neuronal counting experiment, separate control ($n=4$) and BDV-infected ($n=5$) 80-day-old Fisher344 rats were used. These rats were not tested in the neurochemical experiments. The rats were sacrificed as described above. The cerebrum was separated from the cerebellum and hindbrain either for paraffin embedding or frozen sections. Two control and three BDV-infected brains were paraffin-embedded and cut sagittally into 25-$\mu$m thick sections. Two control and two BDV-infected brains were postfixed for 24 h, cryoprotected, frozen, and cut sagittally into 60-$\mu$m sections. The numbers of neurons in the striatum were determined in the right hemisphere for each animal. The fractionator sampling scheme and optical dissector were used to quantitatively measure the numbers of neurons in the striatum (West, 1993). These measurements were performed using an Olympus microscope with a computer driven *x*, *y*, *z*-stage controller (ASI, Eugene, OR) and stereology software (Stereologer; SPA, Alexandria, VA). Ten to 15 sagittal sections through the striatum were selected using a systematic random sampling scheme (e.g., every 6th to 8th section with a random start beginning from the most lateral tissue section). Sections were stained with cresyl violet and viewed at a magnification of 46× and the entire striatum outlined as the region of interest. The borders of the striatum were defined according to the rat atlas of Paxinos and Watson (1986). Estimates of the numbers of neurons were made by counting neurons within a defined volume in each region using an optical dissector. The dimensions of the optical dissector for striatal neurons were: height 12.00 $\mu$m; guard height 2 $\mu$m, spacing 1250 $\mu$m. The coefficient of error (CE) was below 10% for all the animals. To count neurons, an image of counting regions was displayed on the video monitor and a square counting box superimposed on the image using the stereology software Stereologer (SPA). Sections were viewed with a 100× objective (final magnification on the computer screen: 2200×). The depth of the box was measured with the *z*-axis encoder attached to the focusing knob. Nomarski optics were used to optically section the tissue within the box. The nuclei of neurons are darkly stained with cresyl violet, so the nucleus was used as the criterion for determining if a neuron should be counted. A neuron was counted if the top of its nuclei came into focus within the box or touched the top and the right edges of the square frame or the lower surface of the box. Nuclei that touched the bottom and the left edges of the box and the upper surface of the box were excluded. The brain hemispheres used for counting neurons were also used for measuring the volumes of the striatum. The volume of the striatum neocortex was estimated in each rat with Cavalieri point counting using the stereology software Stereologer (SPA). The striatal volumes are expressed as a percentage of the mean control volume for brains processed in either paraffin or frozen tissue

sections. This is to correct for differential shrinkage between paraffin and frozen tissue sections when the sections dry. The average coefficient of variance for the volume estimates in rats was less than 0.05.

*Statistical analysis*
The effects of neonatal BDV infection on the levels of each amino acid were analyzed with Student *t* test. The effects of the compounds on the levels of the amino acids in the perfusates were analyzed with one-way analysis of variance (ANOVA). The effects of neonatal BDV infection on the expression of the GLU transporters and on the total number of neurons and the volume of the striatum were analyzed using Student *t* test. The level of significance was set at $\alpha < .05$.

## References

Alexander GM, Deitch JS, Seeburger JL, Del Valle L, Heiman-Patterson TD (2000). Elevated cortical extracellular fluid glutamate in transgenic mice expressing human mutant (G93A) Cu/Zn superoxide dismutase. *J Neurochem* **74:** 1666–1673.

Anderson CM, Swanson RA (2000). Astrocyte glutamate transport: review of properties, regulation, and physiological functions. *Glia* **32:** 1–14.

Baker DA, Xi ZX, Shen H, Swanson CJ, Kalivas PW (2002). The origin and neuronal function of in vivo nonsynaptic glutamate. *J Neurosci* **22:** 9134–9141.

Bautista JR, Rubin SA, Moran TH, Schwartz GJ, Carbone KM (1995). Developmental injury to the cerebellum following perinatal borna disease virus infection. *Brain Res Dev Brain Res* **90:** 45–53.

Billaud JN, Ly C, Phillips TR, de la Torre JC (2000). Borna disease virus persistence causes inhibition of glutamate uptake by feline primary cortical astrocytes. *J Virol* **74:** 10438–10446.

Briese T, Hornig M, Lipkin WI (1999). Bornavirus immunopathogenesis in rodents: models for human neurological diseases. *J NeuroVirol* **5:** 604–612.

Carbone KM, Park SW, Rubin SA, Waltrip RW 2nd, Vogelsang GB (1991). Borna disease: association with a maturation defect in the cellular immune response. *J Virol* **65:** 6154–6164.

Chen Y, Swanson RA (2003). Astrocytes and brain injury. *J Cereb Blood Flow Metab* **23:** 137–149.

Danbolt NC (2001). Glutamate uptake. *Prog Neurobiol* **65:** 1–105.

de la Torre JC (2002). Bornavirus and the brain. *J Infect Dis* **186(Suppl 2):** S241–S247.

Deitch JS, Alexander GM, Del Valle L, Heiman-Patterson TD (2002). GLT-1 glutamate transporter levels are unchanged in mice expressing G93A human mutant SOD1. *J Neurol Sci* **193:** 117–126.

Dietz D, Vogel M, Rubin S, Moran T, Carbone K, Pletnikov M (2004). Developmental alterations in serotoninergic neurotransmission in Borna disease virus (BDV)-infected rats: a multidisciplinary analysis. *J Neurovirol* **10:** 267–277.

Eisenman LM, Brothers R, Tran MH, Kean RB, Dickson GM, Dietzschold B, Hooper DC (1999). Neonatal borna disease virus infection in the rat causes a loss of purkinje cells in the cerebellum. *J NeuroVirol* **5:** 181–189.

Espey MG, Kustova Y, Sei Y, Basile AS (1998). Extracellular glutamate levels are chronically elevated in the brains of LP-BM5-infected mice: a mechanism of retrovirus-induced encephalopathy. *J Neurochem* **71:** 2079–2087.

Gochenauer GE, Robinson MB (2001). Dibutyryl-cAMP (db-cAMP) up-regulates astrocytic chloride-dependent L-[$^3$H]glutamate transport and expression of both system xc(−) subunits. *J Neurochem* **78:** 276–286.

Gonzalez-Dunia D, Sauder C, de la Torre JC (1997). Borna disease virus and the brain. *Brain Res Bull* **44:** 647–664.

Gonzalez-Dunia D, Watanabe M, Syan S, Mallory M, Masliah E, De La Torre JC (2000). Synaptic pathology in borna disease virus persistent infection. *J Virol* **74:** 3441–3448.

Gonzalez-Dunia D, Volmer R, Mayer D, Schwemmle M. (2005). Borna disease virus interference with neuronal plasticity. *Virus Res* **111:** 224–234.

Gosztonyi G, Ludwig H (1984). Neurotrasnmitter receptors and vial neurotropism. *Neuropsychiatr Clin* **3:** 107–114.

Gosztonyi G, Ludwig H (1995). Borna disease—neuropathology and pathogenesis. *Curr Top Microbiol Immunol* **190:** 39–73.

Gosztonyi G, Ludwig, H (2001). Interaction of viral proteins with neurotransmitter receptors may protect or destroy neurons. *Curr Top Microbiol Immunol* **253:** 121–144.

Haas B, Becht H, Rott R (1986). Purification and properties of an intranuclear virus-specific antigen from tissue infected with Borna disease virus. *J Gen Virol* **67(Pt 2):** 235–241.

Hara MR, Snyder SH (2006). Cell signaling and neuronal death. *Annu Rev Pharmacol Toxicol.*

Hornig M, Chian D, Sindelar M, Hoffman K, Lipkin WI (2001). AMPA receptor disturbances and apoptosis in a rodent model of neurodevelopemtnal damage. Program, 1st Annual International Meeting for Autism Research, San Diego, CA, 2001, p B-49, Abstract no. 21.02.

Hornig M, Weissenböck H, Horscroft N, Lipkin WI (1999). An infection-based model of neurodevelopmental damage. *Proc Natl Acad Sci U S A* **96:** 12102–12107.

Kaul M, Lipton SA (2006). Mechanisms of neuronal injury and death in HIV-1 associated dementia. *Curr HIV Res* **4:** 307–318.

Maragakis NJ, Rothstein JD (2004). Glutamate transporters: animal models to neurologic disease. *Neurobiol Dis* **15:** 461–473.

McBean GJ (2002). Cerebral cystine uptake: a tale of two transporters. *Trends Pharmacol Sci* **23:** 299–302.

Melendez RI, Vuthiganon J, Kalivas PW (2005). Regulation of extracellular glutamate in the prefrontal cortex: Focus on the cystine glutamate exchanger and group I metabotropic glutamate receptors. *J Pharmacol Exp Ther* **314:** 139–147.

Mitchell IJ, Cooper AJ, Griffiths MR (1999). The selective vulnerability of striatopallidal neurons. *Prog Neurobiol* **59:** 691–719.

Nyitrai G, Kekesi KA, Juhasz G (2006). Extracellular level of GABA and Glu: in vivo microdialysis-HPLC measurements. *Curr Top Med Chem* **6:** 935–940.

Pasantes-Morales H (1996). Volume regulation in brain cells: cellular and molecular mechanisms. *Metab Brain Dis* **11:** 187–204.

Paxinos, Watson (1986). *The rat brain in stereotaxic coordinates*, 2nd ed. New York: Academic Press.

Pletnikov MV, Moran TH, Carbone KM (2002a). Borna disease virus infection of the neonatal rat: Developmental brain injury model of autism spectrum disorders. *Front Biosci* **7:** d593–d607.

Pletnikov MV, Rubin SA, Vogel MW, Moran TH, Carbone KM (2002b). Effects of genetic background on neonatal borna disease virus infection-induced neurodevelopmental damage. I. brain pathology and behavioral deficits. *Brain Res* **944:** 97–107.

Richt JA, Rott R (2001). Borna disease virus: a mystery as an emerging zoonotic pathogen. *Vet J* **161:** 24–40.

Sauder C, de la Torre JC (1999). Cytokine expression in the rat central nervous system following perinatal borna disease virus infection. *J Neuroimmunol* **96:** 29–45.

Sonsalla PK, Albers DS, Zeevalk GD (1998). Role of glutamate in neurodegeneration of dopamine neurons in several animal models of parkinsonism. *Amino Acids* **14:** 69–74.

Tang XC, Kalivas PW (2003). Bidirectional modulation of cystine/glutamate exchanger activity in cultured cortical astrocytes. *Ann N Y Acad Sci* **1003:** 472–475.

Timmerman W, Westerink BH (1997). Brain microdialysis of GABA and glutamate: what does it signify? Synapse **27:** 242–261.

Tomonaga K, Kobayashi T, Ikuta K (2002). Molecular and cellular biology of borna disease virus infection. *Microbes Infect* **4:** 491–500.

Weissenböck H, Hornig M, Hickey WF, Lipkin WI (2000). Microglial activation and neuronal apoptosis in bornavirus infected neonatal lewis rats. *Brain Pathol* **10:** 260–272.

West MJ (1993). New stereological methods for counting neurons. *J Neuropathol Exp Neurol* **14:** 275–285.

Williams BL, Lipkin WI (2006). Endoplasmic reticulum stress and neurodegeneration in rats neonatally infected with borna disease virus. *J Virol* **80:** 8613–8626.